Dalton Transactions

ROYAL SOCIETY OF CHEMISTRY

PAPER

View Article Online
View Journal | View Issue

Cite this: *Dalton Trans.*, 2025, **54**, 5708

Luminescence enhancement by mixing carboxylate benzoate–pentafluorobenzoate ligands in polynuclear $\{Eu_2Zn_2\}$ and $\{Tb_2Zn_2\}$ complexes†

Alena E. Bolot'ko, *[a,b] Maxim A. Shmelev, [a] Alexandr S. Chistyakov,[a] Julia K. Voronina, [a] Evgeniya A. Varaksina,[c] Natalia V. Gogoleva,[a] Ilya V. Taydakov, [c] Alexey A. Sidorov[a] and Igor L. Eremenko [a]

Received 9th December 2024,
Accepted 28th February 2025

DOI: 10.1039/d4dt03414g

rsc.li/dalton

This study investigates mixed-carboxylate benzoate (bz)–pentafluorobenzoate (pfb) $\{Eu_2Zn_2\}$ and $\{Tb_2Zn_2\}$ compounds with 1,10-phenanthroline (phen) molecules. It is demonstrated that variation of the synthesis conditions yields mixed-carboxylate compounds with different compositions: $[Ln_2Zn_2(phen)_2(bz)_{5.2}(pfb)_{4.8}]$ (Ln = Eu ($\mathbf{1_{Eu}}$), Tb ($\mathbf{1_{Tb}}$)) and $[Eu_2Zn_2(phen)_2(bz)_4(pfb)_6]\cdot 4MeCN$ ($\mathbf{2_{Eu}}$). In these structures, bz^- and pfb^- anions occupy specific positions in various ratios. Benzoate compounds $[Ln_2Zn_2(phen)_2(bz)_{10}]$ (Ln = Eu ($\mathbf{3_{Eu}}$), Tb ($\mathbf{3_{Tb}}$)) were synthesized in order to compare the structures and photoluminescence properties of complexes **1** and **2** with their homoanionic analogues, and comparison was also made with previously reported pentafluorobenzoate complexes $[Ln_2Zn_2(pfb)_{10}(phen)_2]$ (Ln = Eu ($\mathbf{4_{Eu}}$), Tb ($\mathbf{4_{Tb}}$)). It was found that the introduction of a second type of anion into the studied compounds improves the photoluminescence properties and alters the geometry of the metal core, the polyhedra of rare-earth elements (REEs), and the system of non-covalent interactions compared to benzoate and pentafluorobenzoate complexes.

Introduction

Luminescent lanthanide complexes have attracted significant attention due to their potential applications in producing luminescent sensors, lasers, diodes, catalysis, and biomedical imaging.[1–6] They are also considered as single-molecule magnets for a new generation of high-density information storage and ultra-fast processing devices.[7–11] Development of effective methods to improve the luminescence properties of coordination compounds remains a critical practical challenge. The rational selection of the ligand environment surrounding the lanthanide ion determines the structure of the coordination compound, the efficiency of luminescence sensitization of the lanthanide ion, and the probability of luminescence quenching.[12–15]

The incorporation of a d-block ion, such as Zn^{2+} or Cd^{2+}, with organic antenna molecules into the coordination environment of a lanthanide ion can also influence the luminescence efficiency of the compounds by inducing structural modification, altering the geometry of the coordination polyhedron of the metal ions, and minimizing the interionic interactions.[16–20]

The simultaneous incorporation of multiple different ionic co-ligands into a lanthanide compound can result in structural modifications and a significant increase in photoluminescence properties.[21–24] For example, in europium compounds, it has been demonstrated that the combination of three ligands within a single complex can lead to a fivefold increase in luminescence efficiency.[25] Similarly, the use of four ionic ligands in the synthesis of a samarium complex resulted in a compound with a record quantum yield of luminescence for this metal ion.[26] While these studies have established a promising foundation, no investigations have yet explored how the ratio of ligands in the composition of such compounds affects their structure and photoluminescence properties, leaving the factors influencing these properties only partially understood.

[a]*N. S. Kurnakov Institute of General and Inorganic Chemistry, Russian Academy of Sciences, Leninsky Prospect 31, 119991 Moscow, Russian Federation. E-mail: al.bolotko@gmail.com*

[b]*Faculty of Chemistry of the Higher School of Economics, Vavilova st, 7, 117312 Moscow, Russian Federation*

[c]*P.N. Lebedev Physical Institute of the Russian Academy of Sciences, Leninsky Prospect 53, 119991 Moscow, Russian Federation*

†Electronic supplementary information (ESI) available: PXRD patterns for $\mathbf{1_{Eu}}$, $\mathbf{1_{Tb}}$, $\mathbf{2_{Eu}}$, and $\mathbf{3_{Eu}}$; continuous shape measures (CShM) for Zn and Ln coordination polyhedra; tables of hydrogen bonds and C–F···π and C–N···π interaction parameters; main crystallography data and refinement details; emission spectra of **1**–**4** at 300 K and 77 K and excitation spectra of **1**–**4** at 300 K and 77 K. CCDC 2343086 ($\mathbf{1_{Eu}}$), 2343087 ($\mathbf{1_{Tb}}$), 2343088 ($\mathbf{2_{Eu}}$), 2390847 ($\mathbf{3_{Eu}}$). For ESI and crystallographic data in CIF or other electronic format see DOI: https://doi.org/10.1039/d4dt03414g

This work aimed at studying mixed-carboxylate $\{Eu_2Zn_2\}$ and $\{Tb_2Zn_2\}$ compounds containing anions of benzoic acid (H(bz)) and pentafluorobenzoic acid (H(pfb)), as well as 1,10-phenanthroline molecules, and comparing their structures and photoluminescence properties with those of homoanionic pentafluorobenzoate and benzoate analogues. The combination of perfluorinated and non-fluorinated aromatic anions in the structure of a coordination compound can result in the formation of multiple non-covalent interactions.[27] Such systems are characterized by the formation of a dense stacked arrangement of aromatic rings, with their distances approaching 3.4–3.6 Å due to "arene–perfluoroarene" interactions, which involve contributions from various non-covalent forces (π···π, C–F···π, C–H···F, *etc.*). These interactions can significantly influence the molecular and crystalline structures of the resulting compounds.[28–32]

Results and discussion

Synthesis of complexes

To obtain mixed-carboxylate zinc and lanthanide complexes, benzoate and pentafluorobenzoate salts of the corresponding metals were used: $[Zn(pfb)_2(H_2O)]$,[33] $[Zn(bz)_2(H_2O)_2]\cdot Hbz$,[34] $[Ln_2(pfb)_6(H_2O)_8]\cdot 2H_2O$ (Ln = Eu, Tb),[35] and $[Ln(bz)_3(H_2O)_4]$ (Ln = Eu, Tb),[36] which were synthesized using previously described methods.

It was found that the composition of the mixed-carboxylate complexes in this case changes depending on the metal salt used in the synthesis. In the reaction of zinc pentafluorobenzoate, rare-earth benzoate, and 1,10-phenanthroline (in a 1 : 1 : 1 ratio, with the anion ratio bz : pfb = 3 : 2) in acetonitrile, crystals of the compound $[Ln_2Zn_2(phen)_2(bz)_{5.2}(pfb)_{4.8}]$ (Scheme 1, Ln = Eu ($\mathbf{1_{Eu}}$), Tb ($\mathbf{1_{Tb}}$)) were obtained. Replacing the initial salts with zinc benzoate and europium pentafluorobenzoate, in a reaction with 1,10-phenanthroline (1 : 1 : 1 ratio, with the anion ratio bz : pfb = 2 : 3) in acetonitrile, led to the formation of crystals of $[Eu_2Zn_2(phen)_2(bz)_4(pfb)_6]\cdot 4MeCN$ composition (Scheme 1, $\mathbf{2_{Eu}}$).

The structure of the obtained tetranuclear complex **1** contains four benzoate anions, two pentafluorobenzoate anions, and four positions in which bz and pfb anions are simultaneously refined, with a ratio of 0.3 : 0.7, according to single-crystal X-ray diffraction (SCXRD) data. The occupancies of the disordered anions were determined during the refinement of

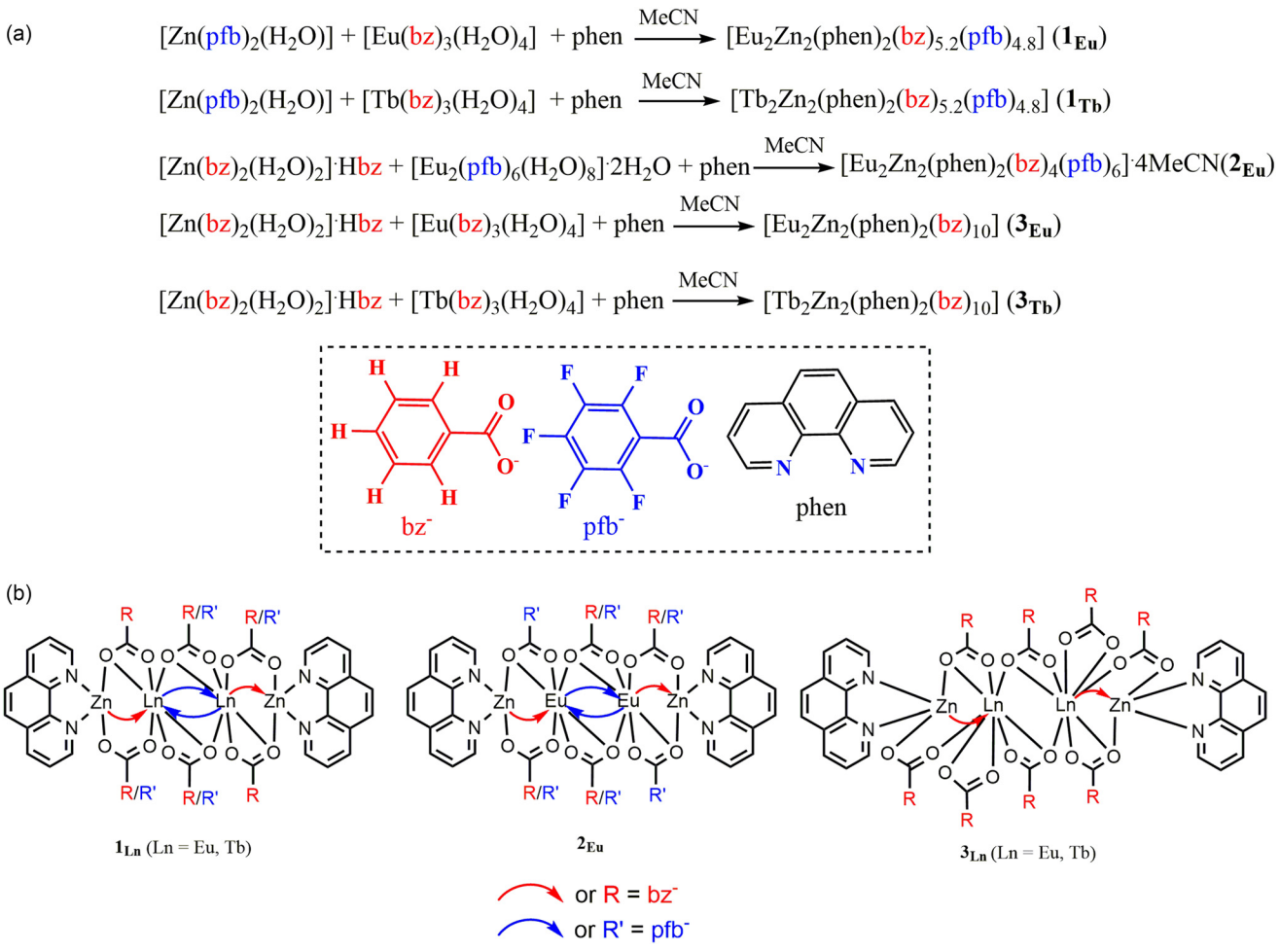

Scheme 1 Synthesis (a) and structural formulas (b) of complexes **1–3**.

SCXRD data using free variables, subsequently fixed to an accuracy of one decimal place, and found to be in good agreement with the results of CHN analysis. The phase purity of complex **1** was confirmed by powder X-ray diffraction (PXRD) (Fig. S1 and S2†). The reagent ratio in the first reaction (Scheme 1a) could theoretically support the quantitative formation of the heterometallic mixed-carboxylate complex $[Ln_2Zn_2(phen)_2(bz)_6(pfb)_4]$. However, the significant increase in pentafluorobenzoate content in the obtained complex **1** suggests that the expected composition does not correspond to a thermodynamically stable compound. When the reagent ratios were altered and the initial synthesis was repeated, the occupancies of the anion positions in complex **1** $[Ln_2Zn_2(phen)_2(bz)_{5.2}(pfb)_{4.8}]$ were well reproduced, indicating that, despite its nonstoichiometric composition, the product is likely a co-crystal rather than a phase of variable composition or a solid solution.

In the structure of compound $\mathbf{2_{Eu}}$, simultaneous localization of benzoate and pentafluorobenzoate anions is also observed at four anion positions, with ratios of 0.2 : 0.8 and 0.8 : 0.2, respectively. However, according to powder X-ray diffraction (PXRD) data, compound $\mathbf{2_{Eu}}$ is not phase-pure and contains impurities that could not be identified (Fig. S3†).

When the ratio of the initial reagents was altered (zinc salt, europium salt, and 1,10-phenanthroline in ratios of 1 : 2 : 1 or 2 : 1 : 2, respectively), it was not possible to isolate mixed-carboxylate compounds with different compositions. Only crystals of benzoate or pentafluorobenzoate complexes, $[Ln_2Zn_2(phen)_2(bz)_{10}]$ (Ln = Eu($\mathbf{3_{Eu}}$), Tb($\mathbf{3_{Tb}}$)) and $[Ln_2Zn_2(phen)_2(pfb)_{10}]$ (Ln = Eu($\mathbf{4_{Eu}}$), Tb($\mathbf{4_{Tb}}$)), were formed.[37]

To compare the photoluminescence properties of complex **1** with its homoanionic analogue, the previously described complex $[Tb_2Zn_2(phen)_2(bz)_{10}]$ (Scheme 1, $\mathbf{3_{Tb}}$)[38] was synthesized, for which data on quantum yields and luminescence lifetimes were previously unavailable. Additionally, the complex $[Eu_2Zn_2(phen)_2(bz)_{10}]$ (Scheme 1, $\mathbf{3_{Eu}}$) was synthesized for the first time. The phase purity of complexes **3**, as well as the isostructurality of complex $\mathbf{3_{Tb}}$ to the previously described complex $\mathbf{3_{Eu}}$, was confirmed by powder X-ray diffraction (PXRD) (Fig. S4 and S5†). A comparison of the structures of compounds **1** and $\mathbf{2_{Eu}}$ with the previously obtained pentafluorobenzoate complexes $[Ln_2Zn_2(phen)_2(pfb)_{10}]$ (Ln = Eu($\mathbf{4_{Eu}}$), Tb ($\mathbf{4_{Tb}}$))[37] was also made.

Using IR spectroscopy, the primary composition of the resulting compounds was confirmed (S6–S10†). Complexes $\mathbf{1_{Eu}}$, $\mathbf{1_{Tb}}$, and $\mathbf{2_{Eu}}$ are heteroanion compounds containing pfb- and bz-anions, whereas complexes $\mathbf{3_{Eu}}$ and $\mathbf{3_{Tb}}$ are homoanion compounds with only bz–anions. All the complexes contain 1,10-phenanthroline ligand molecules. Characteristic peaks corresponding to the out-of-plane skeletal bending of the aromatic system were observed in the range of 714–720 cm^{-1}. Peaks associated with the out-of-plane C–H vibrations of the condensed aromatic system appear in the range of 837–847 cm^{-1}, while skeletal stretching vibrations are located in the range of 1516–1520 cm^{-1}.

For complexes $\mathbf{1_{Eu}}$, $\mathbf{1_{Tb}}$, and $\mathbf{2_{Eu}}$, which contain pfb acid anions, intense vibrations of the aromatic system of this acid are observed at 1490–1491 cm^{-1}. However, similar vibration peaks from the bz acid anions were found in all the obtained complexes, located in the range of 1558–1561 cm^{-1}. Additionally, in complexes $\mathbf{1_{Eu}}$, $\mathbf{1_{Tb}}$, and $\mathbf{2_{Eu}}$, skeletal C–F vibration bands were observed at 991 cm^{-1}. The most intense peaks correspond to the vibrations of the carboxylate groups of the acid anions, located in the regions of 1600–1603 cm^{-1} for asymmetric vibrations and 1394–1398 cm^{-1} for symmetric vibrations.

The structure of complexes

The obtained compounds **1–3** are molecular complexes based on a tetrahedral Zn–Ln–Ln–Zn metal core, where bz – and/or pfb anions function as bridging ligands, and phenanthroline molecules are bidentately coordinated to the terminal zinc atoms. The metal ions and phenanthroline molecules form a plane, relative to which the molecular geometry can be conveniently analyzed.

The zinc and rare-earth ions in the structures of complexes **1–3** are linked by two bridging anions and one chelating–bridging carboxylate anion (Fig. 1). One of the bridging anions adopts an almost planar conformation and forms in the main plane of the molecule (Zn1–O3–O4–Eu1, the maximum deviation from the plane is observed in complex $\mathbf{3_{Eu}}$, where the oxygen atom O4 is displaced from the plane by 0.111(6) Å). The maximum deviations from the plane in the molecules of the remaining compounds are within the margin of error (Fig. S11†). The carboxyl groups of the second bridging and chelating–bridging carboxylate anions are positioned above and below the main plane at angles close to 90°, with the aromatic fragments of the anions rotated relative to their respective carboxyl groups. The zinc ions in all the complexes are in a distorted octahedral environment (Fig. 2 and S12†), formed by four oxygen atoms from the carboxylate anions and two nitrogen atoms from the phenanthroline moiety (Table S4,† ZnO_4N_2 CShM($\mathbf{1_{Eu}}$) = 2.792; CShM($\mathbf{1_{Tb}}$) = 2.774, CShM($\mathbf{2_{Eu}}$) = 2.577, CShM($\mathbf{3_{Eu}}$) = 2.990).

Four carboxylate anions are localized between the rare-earth ions in all complexes, two of which act as chelating–bridging ligands in all studied complexes and are positioned almost perpendicular to the main molecular plane. The other two anions, found in complexes $\mathbf{1_{Eu}}$, $\mathbf{1_{Tb}}$, and $\mathbf{2_{Eu}}$, and the previously described $\mathbf{4_{Eu}}$ and $\mathbf{4_{Tb}}$, which contain pfb anions, coordinate in the main plane and serve as bridging ligands. In the benzoate complex $\mathbf{3_{Eu}}$, these two anions are coordinated as chelating to each rare-earth ion. As a result, the coordination polyhedra of the eight-coordinated rare-earth ions in the studied complexes differ, forming a square anti-prism in the pfb complexes $\mathbf{1_{Eu}}$, $\mathbf{1_{Tb}}$, and $\mathbf{2_{Eu}}$ (LnO_8, CShM($\mathbf{1_{Eu}}$) = 1.131); CShM($\mathbf{1_{Tb}}$) = 1.108, CShM($\mathbf{2_{Eu}}$) = 1.223, and a biaugmented trigonal prism (LnO_8, CShM($\mathbf{3_{Eu}}$) = 3.515) in the bz complex $\mathbf{3_{Eu}}$ (Fig. 2 and S12†).

Such a difference in the coordination pattern and polyhedron type leads to a change in the metal core. Thus, the distance between the rare-earth ions is expected to be the greatest in complex $\mathbf{3_{Eu}}$, slightly smaller in $\mathbf{1_{Eu}}$, and minimal in $\mathbf{2_{Eu}}$

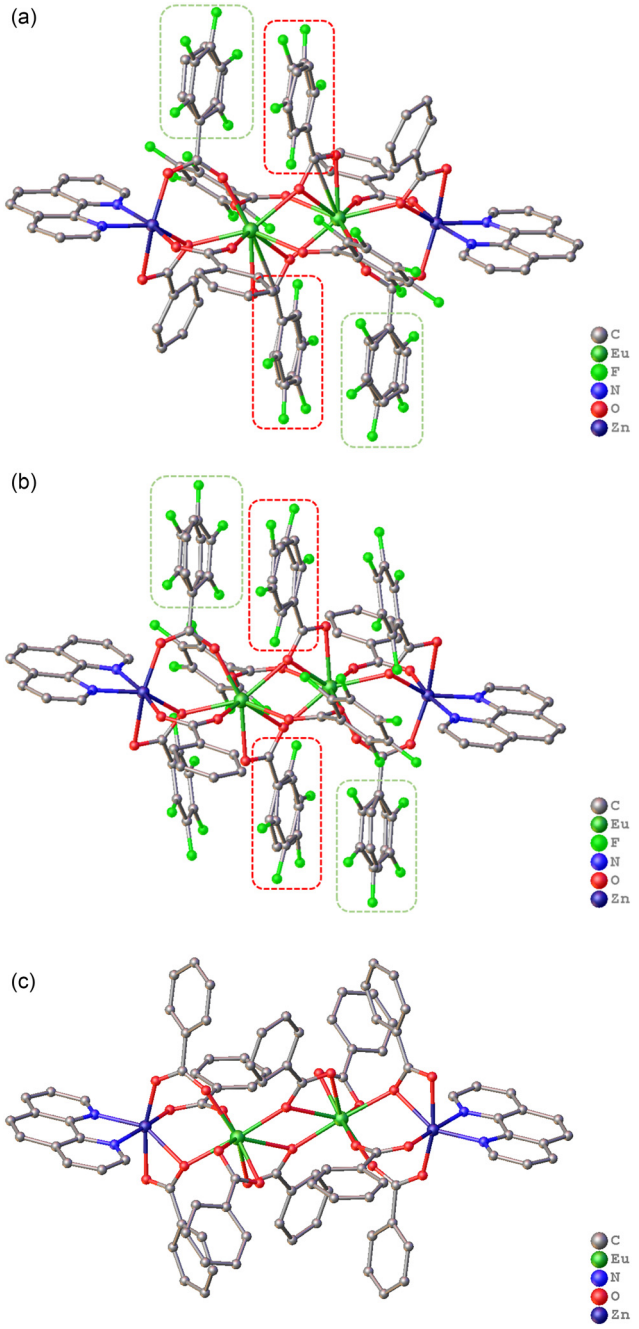

Fig. 1 Molecular structure of Eu_2Zn_2 complexes $\mathbf{1}_{Eu}$ (a), $\mathbf{2}_{Eu}$ (b) and $\mathbf{3}_{Eu}$. Dashed lines indicate pfb/bz anions with disordered positions. Solvent molecules and H-atoms omitted for clarity.

(Table 1). This change correlates with the number of benzoate anions in the molecule; the fewer are the benzoate anions, the shorter is the distance between the lanthanides. It is interesting to note that the corresponding distance in the pfb complex $\mathbf{4}_{Eu}$ is about 4 Å, which would not allow making a conclusion about a direct dependence of the distance between the rare-earth ions on the number of bz anions. However, a detailed analysis of the geometry of complex $\mathbf{4}_{Eu}$ reveals significant differences compared to complexes **1–3**. In particular, the main molecular plane cannot be identified, as the angle between the plane formed by the metal ions and the phenanthroline planes is 24.1(1)°. Additionally, the complex contains no anions with a planar structure.

In the final refinement of SCXRD data, it was found that the thermal parameters of the fluorine atoms in the pentafluorobenzoate anions, which occupy two positions in compounds **1** and $\mathbf{2}_{Eu}$, were elongated. The corresponding ellipsoids were stretched along the C–F bond direction, indicating disorder in the pentafluorobenzoate fragment, which is distributed between two positions. Several attempts to refine the structures with this disorder were made but proved to be unsuccessful. Since this phenomenon was observed during the refinement of experimental data obtained for several crystals from the same sample, it became evident that the issue was unrelated to crystal quality or inaccuracies in data acquisition or refinement. Significant improvement in the experimental results was achieved by refining the occupancies of the corresponding fluorine atoms as free variables. As a result, the occupancies of all fluorine atoms in each disordered pfb ring were found to be consistent. This led us to hypothesize that the second component might not be fluorine atoms but rather hydrogen atoms, suggesting that the corresponding positions were occupied by a mixture of pentafluorobenzoic acid and benzoic acid anions in a specific ratio. Refinement of the corresponding models equalized the thermal parameters of all atoms and significantly reduced the *R*-factor values, confirming the validity of the structure solution.

Thus, the structures of compounds $\mathbf{1}_{Eu}$, $\mathbf{1}_{Tb}$, and $\mathbf{2}_{Eu}$ represent mixed-carboxylate complexes in which bz^- and pfb^- anions are refined in four positions (two in the independent part of the unit cell) with varying ratios, indicating the simultaneous presence of molecules with different compositions within the crystal. In other words, the crystals of $\mathbf{1}_{Eu}$, $\mathbf{1}_{Tb}$, and $\mathbf{2}_{Eu}$ are co-crystals of complexes where four anions, acting as bridging ligands between zinc and lanthanide ions and as chelating–bridging ligands between lanthanide ions, are either bz^- or pfb^-. Since SCXRD data represent an averaged superposition of the crystal as a whole, only the ratio of anions at each position can be discussed. Thus, in the crystals of compound **1**, the ratio between fluorinated and non-fluorinated anions is 0.7 : 0.3. In compound $\mathbf{2}_{Eu}$, this ratio varies: in the terminal region, the pfb/bz ratio is 0.8 : 0.2, while in the central region, it is reversed to 0.2 : 0.8.

The presence of disordered anion positions in complexes **1** and $\mathbf{2}_{Eu}$ was unexpected. A review of literature data on crystals of similar organic systems (comprising benzoic acid and its fluorinated derivatives) revealed that disordered anion positions are typically observed only in systems containing monofluorinated or specific isomers of di- or trifluorobenzoic acids.[39] For systems containing benzoic/3,4,5-trifluorobenzoic (tetra- or pentafluorobenzoic) acids, only organic co-crystals with fixed compositions are reported to form.[39,40]

Analysis of molecular packing in the studied crystal structures revealed, as anticipated, that the primary structure-forming interactions are π···π interactions between aromatic

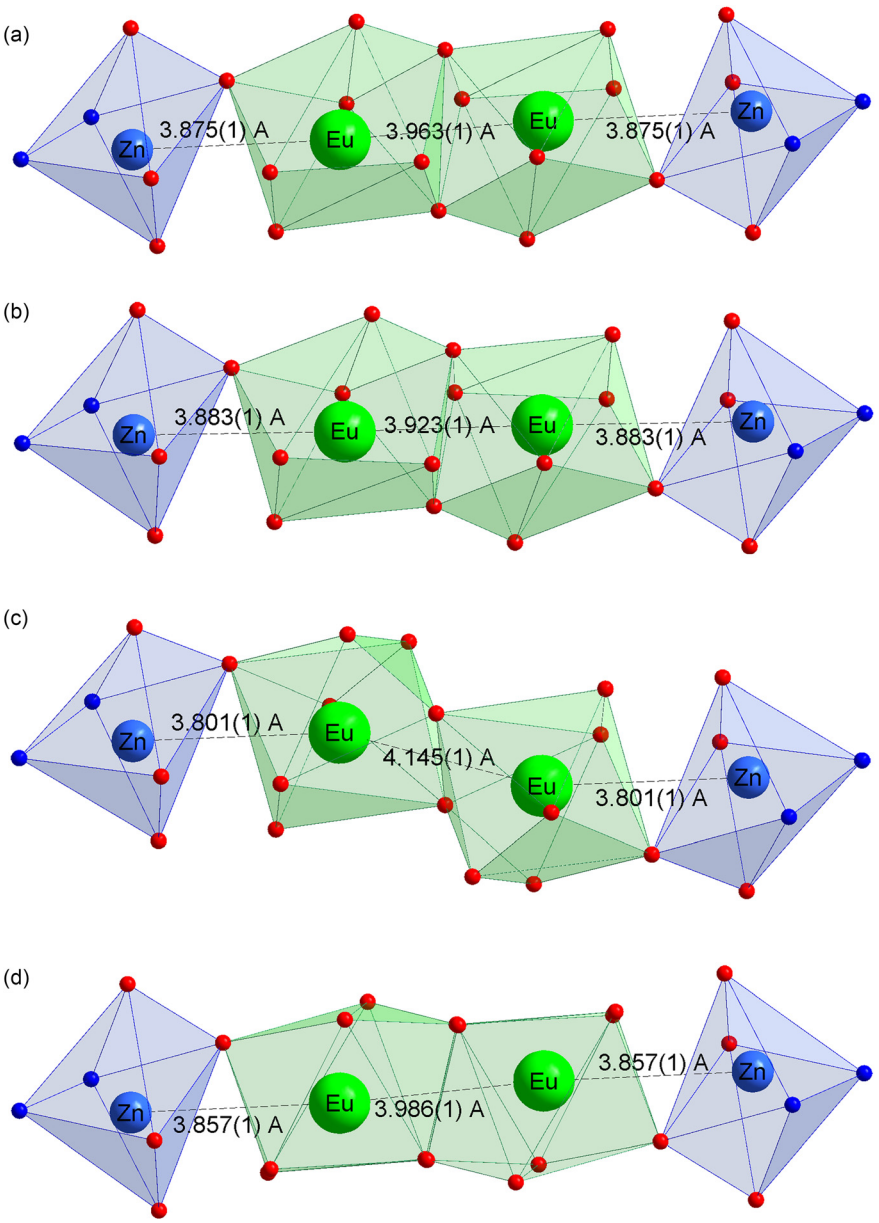

Fig. 2 Coordination polyhedra of Zn and Eu metal ions and metal–metal distances in complexes $\mathbf{1}_{Eu}$ (a), $\mathbf{2}_{Eu}$ (b), $\mathbf{3}_{Eu}$ (c), and $\mathbf{4}_{Eu}$ (d).

Table 1 Basic geometric parameters of the complexes $\mathbf{1}_{Eu}$, $\mathbf{1}_{Tb}$, $\mathbf{2}_{Eu}$, and $\mathbf{3}_{Eu}$

	Distance, Å			
Bond	$\mathbf{1}_{Eu}$	$\mathbf{1}_{Tb}$	$\mathbf{2}_{Eu}$	$\mathbf{3}_{Eu}$
Zn–O	2.029(4)–2.306(4)	2.021(3)–2.293(3)	1.991(6)–2.339(6)	2.025(5)–2.313(6)
Ln–O	2.298(4)–2.589(4)	2.297(3)–2.581(3)	2.284(6)–2.535(3)	2.314(5)–2.637(5)
Zn–N	2.099(5), 2.178(5)	2.101(3), 2.178(4)	2.086(6), 2.146(7)	2.107(6), 2.177(6)
Zn⋯Ln	3.875(1)	3.860(1)	3.883(1)	3.801(1)
Ln⋯Ln	3.963(1)	3.945(1)	3.923(1)	4.145(1)
Angle, °				
Zn–Ln–Ln	162.28(2)	162.42(2)	160.25(2)	146.86(2)

fragments (Fig. 3 and Table 2). In the crystals of complexes $\mathbf{1}_{Eu}$ and $\mathbf{1}_{Tb}$, infinite layers are created through π⋯π stacking interactions between phenanthroline rings, which are aligned parallel to the 0a-axis (Fig. 3(a)). The three-dimensional crystal packing arises due to stacking interactions between the aromatic rings of disordered bz and pfb fragments. In the crystal of complex $\mathbf{2}_{Eu}$, paired π⋯π interactions occur between the phenanthroline and benzoate anion fragments of the molecules, resulting in infinite chains parallel to the b0c-plane (Fig. 3(b)). These chains are further interconnected by weak C–H⋯F and C–F⋯π interactions (Tables S2 and S3†). Additionally, in $\mathbf{2}_{Eu}$, the nitrogen atoms of acetonitrile solvate molecules form short contacts with the disordered aromatic bz/pfb fragments, with centroid distances of 3.50(3)/3.93(2) Å

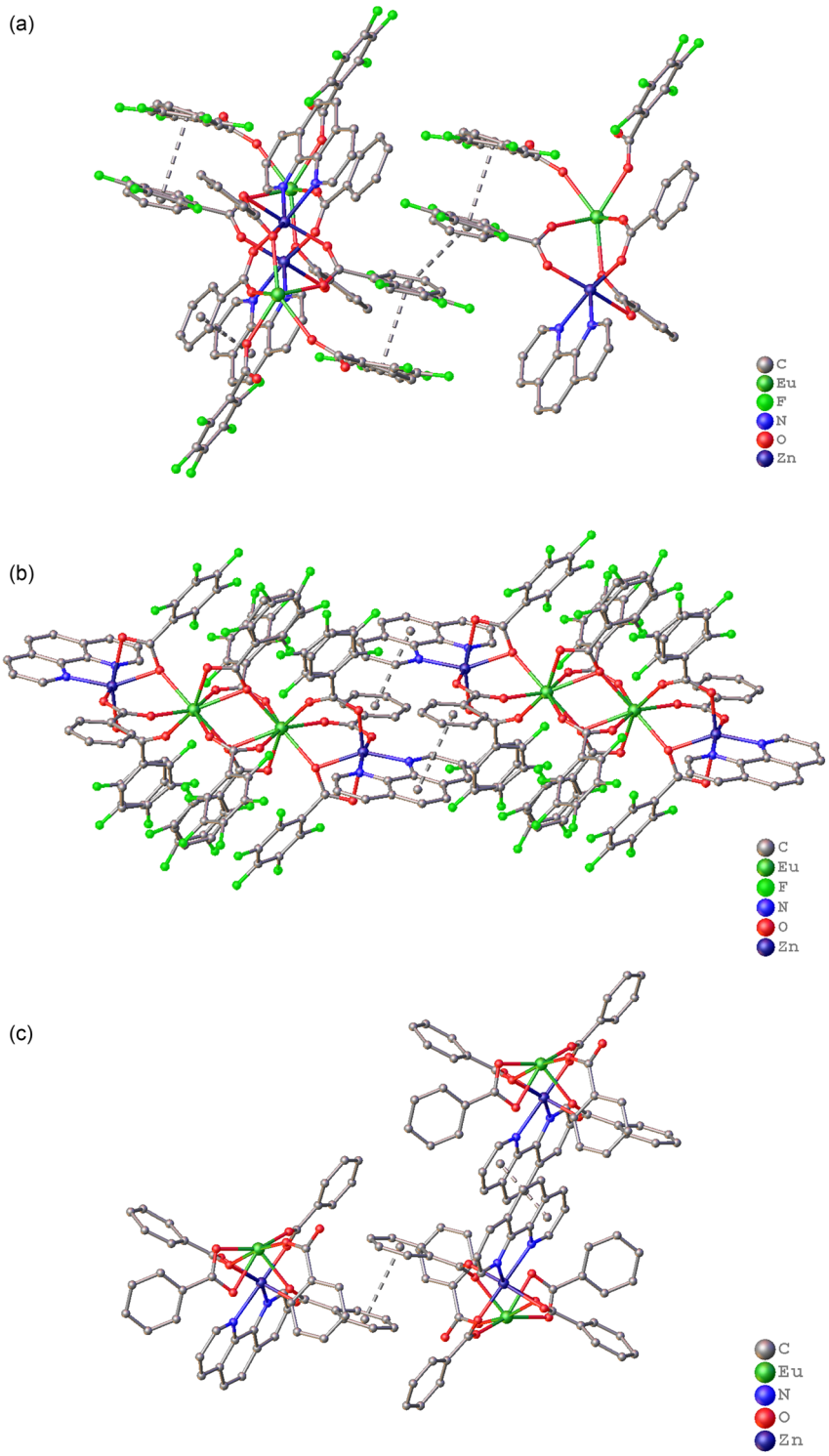

Fig. 3 Fragment of the crystal packing for complexes $\mathbf{1}_{Eu}$ (a), $\mathbf{2}_{Eu}$ (b), and $\mathbf{3}_{Eu}$ (c). Dashed lines indicate π···π interactions. Solvent molecules and H-atoms omitted for clarity.

and angles (γ) of 23.43°/17.02°, suggesting π-system interactions between the aromatic ring and acetonitrile. In the crystal of $\mathbf{3}_{Eu}$, stacking interactions between four aromatic fragments (two central phenanthroline rings and two benzene rings on either side of the phenanthrolines) form an infinite layer parallel to the b0c-plane (Fig. 3(c) and Table 2). These layers are connected through C–H···O interactions (Table S3†). Previously reported pentafluorobenzoate complex **4** forms chains due to π···π interactions between the phenanthroline fragments of neighboring molecules. In addition, acetonitrile

Table 2 Summary of π···π interactions in the crystal packing of complexes $\mathbf{1}_{Eu}$, $\mathbf{1}_{Tb}$, $\mathbf{2}_{Eu}$, and $\mathbf{3}_{Eu}$

Interactions	Cg···Cg, Å	Symmetry code	Cg···Perp, Å	α, °
Complex $\mathbf{1}_{Eu}$				
phen···bz	3.652(4)	$1-x,-y,2-z$	3.326(3)	6.0(4)
phen···bz	3.684(5)	$1-x,-y,2-z$	3.442(3)	5.8(4)
bz/pfb···bz/pfb	3.612(5)		3.301(3)	8.7(4)
Complex $\mathbf{1}_{Tb}$				
phen···bz	3.657(3)	$1-x,-y,2-z$	3.335(2)	6.3(3)
phen···bz	3.697(3)	$1-x,-y,2-z$	3.445(3)	5.6(3)
bz/pfb···bz/pfb	3.605(4)		3.458(3)	8.9(3)
Complex $\mathbf{2}_{Eu}$				
bz/pfb···bz/pfb	3.650(9)	$1-x,-y,1-z$	3.547(7)	6.8(8)
phen···bz	3.687(7)	$1-x,1-y,-z$	3.687(7)	4.3(5)
Complex $\mathbf{3}_{Eu}$				
phen···phen	3.412(5)	$1-x,2-y,1-z$	3.280(4)	0.0(4)
bz···bz	3.638(6)	$-x,1-y,-z$	3.546(4)	0.0(5)

Cg is the centroid of aromatic rings, Perp is a perpendicular to the plane of the ring, and α is the angle between the planes of aromatic fragments.

solvate molecules are integrated into the π···π interaction system, interacting with the phenanthroline of one molecule and the pfb^- anion of another, with the shortest interatomic distances measured at 3.21(2) and 3.289 Å, respectively.[37]

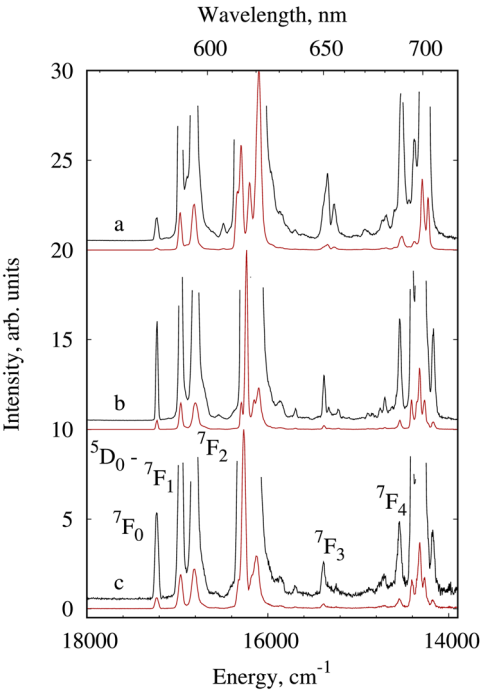

Fig. 4 Luminescence spectra of $\mathbf{4}_{Eu}$ (a), $\mathbf{1}_{Eu}$ (b) and $\mathbf{3}_{Eu}$ (c) at 77 K, λ_{ex} = 280 nm. The black line indicates the spectra at an enlarged scale.

Luminescence properties of complexes

To evaluate the influence of mixed carboxylate ligands on the efficiency of energy transfer processes, the photophysical properties of mixed carboxylate benzoate-pentafluororbenzoate of the compounds **1** benzoate compound **3** were investigated in detail and compared with previously studied compounds $\mathbf{4}_{Eu}$**4and** $_{Tb}$ with pentafluorobenzoic acid anions.[37] The luminescence spectra of the europium complexes $\mathbf{1}_{Eu}$, $\mathbf{3}_{Eu}$ and $\mathbf{4}_{Eu}$ obtained at 300 K and 77 K display line-like luminescence associated with the f–f transition of Eu^{3+} (Fig. S14† and Fig. 4). The singlet transition $^5D_0 \rightarrow {}^7F_0$ at about 580 nm is unique and symmetrical and indicates one type of emission center for each of the compounds studied. The $^5D_0 \rightarrow {}^7F_1$ transition splits into two components which is related to the axial D4d symmetry of the coordination polyhedron obtained by X-ray diffraction data (Table S4†) The transition $^5D_0 \rightarrow {}^7F_2$ is very sensitive to the ligand environment and according to Judd–Ofelt theory is strictly forbidden at the site with the inversion center. In contrast, the transition $^5D_0 \rightarrow {}^7F_1$ is allowed by the Laporte selection rules and its integrated intensity does not depend on the environment in the first approximation. This property is often used to compare the emission spectra of different europium complexes. The ratio of the $^5D_0 \rightarrow {}^7F_2$ transition to the magnetic dipole transition $^5D_0 \rightarrow {}^7F_1$ is 4.48 for $\mathbf{1}_{Eu}$, 4.08 for $\mathbf{3}_{Eu}$ and 5.97 for $\mathbf{4}_{Eu}$, which indicate that the Eu^{3+} ion site is non-centrosymmetric. A similar pattern of Stark splitting of the f–f transition indicates roughly the same charge distribution in the inner coordination sphere of the europium ion for the complexes $\mathbf{1}_{Eu}$ and $\mathbf{3}_{Eu}$ while for complex $\mathbf{4}_{Eu}$ it has some differences.

The terbium complexes $\mathbf{4}_{Tb}$, $\mathbf{1}_{Tb}$ and $\mathbf{3}_{Tb}$ under ligand excitation and at 77 K exhibit the characteristic luminescence from the $^5D_4$ level of the terbium ion (Fig. 5). The highest intensity was detected for the transition $^5D_4 \rightarrow {}^7F_5$ located in the spectral range of 535–555 nm. Three transitions $^5D_4 \rightarrow {}^7F_{2-0}$ have an extremely low intensity typical of terbium complexes. In contrast to europium complexes, the splitting pattern of the $^5D_4 \rightarrow {}^7F_5$ transition of Tb^{3+} seems quite similar for three terbium compounds. However, due to the large value of the quantum number J of the initial and final state of Tb^{3+}, a huge number of overlapping spectral bands are observed when degeneracy is removed by a crystal field. For the terbium compounds studied, detailed comparison of the spectral band splitting is complicated even at low temperature.

The broadband emission in the 340–450 nm spectral range is clearly observed in the emission spectra of the investigated compounds (Fig. S15†). The observed bands are typical of heteronuclear compounds and early were associated with the luminescence of d-block.[41] The presence of the ligand emission indicates incomplete energy transfer to the lanthanide ion. To estimate the energy losses, the ratio of the d-block luminescence intensity to the intensity of the lanthanide luminescence band ($^5D_4 \rightarrow {}^7F_5$ and $^5D_0 \rightarrow {}^7F_1$ for terbium and europium complexes, respectively) was calculated. The obtained ratios are 0.12, 0.05 and 0.22 for $\mathbf{3}_{Tb}$, $\mathbf{1}_{Tb}$ and $\mathbf{4}_{Tb}$ and 1.07, 0.41 and 0.64 for $\mathbf{3}_{Eu}$, $\mathbf{1}_{Eu}$ and $\mathbf{4}_{Eu}$, respectively. It can be noted that the relative intensity of broadband luminescence of heteroanionic compounds is noticeably lower than that of homoanionic compounds, which indicates lower energy losses

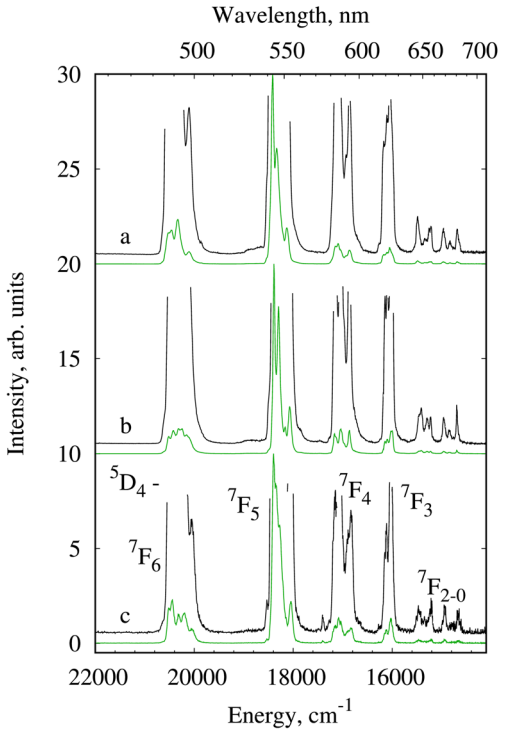

Fig. 5 Luminescence spectra of $\mathbf{4}_{\mathbf{Tb}}$ (a), $\mathbf{1}_{\mathbf{Tb}}$ (b) and $\mathbf{3}_{\mathbf{Tb}}$ (c) at 77 K, λ_{ex} = 280 nm. The black line indicates the spectra in an enlarged scale.

during energy transfer to the lanthanide ion in mixed carboxylate compounds.

The excitation spectra of compounds **1** and **3** obtained at 300 K and 77 K are presented in Fig. S14 and S16.† The long-wavelength maximum of the broadband excitation line located at 345 nm can be associated with absorption of the 1,10-phenantroline ligand which is an effective and widely used sensitizer for excitation of europium and terbium ions.[42] The excitation spectrum of the complex $\mathbf{4}_{\mathbf{Eu}}$ contains a weak shoulder in the wavelength range 340–390 nm, which is absent in the isostructural terbium complex and can be assigned to a ligand-to-metal charge transfer (LMCT) state.

The absolute quantum yield of lanthanide-centered emission for $\mathbf{3}_{\mathbf{Eu}}$ is the lowest in the series of investigated complexes which may partially be due to weak quenching of the excited state of Eu^{3+} by the CH high-energy oscillator of the bz anion (Table 3). A gradual decrease in the nonradiative rate constant A_{rad} occurs when bz is replaced by the pfb anion. In addition, compounds $\mathbf{4}_{\mathbf{Eu}}$ and $\mathbf{4}_{\mathbf{Tb}}$ show a slight increase in the observed luminescence lifetime compared to compounds **1** and **3**. However, the best quantum yield is observed for compounds **1** containing both bz and pfb anions. According to the sensitization efficiency values for europium compounds, mixed carboxylate compounds provide better energy transfer to the lanthanide ion than homoanionic compounds. This effect may be associated with a significant restructuring of the system of non-covalent interactions during the formation of a heteroanionic complex. As indicated above, the lowest energy losses for the luminescence of the d-block are observed for the heteroanion complex, which contributes to a more efficient transfer of excitation to the lanthanide ion. Moreover, a significant decrease in the sensitization efficiency for the complex $\mathbf{4}_{\mathbf{Eu}}$ is due to energy quenching by the low-lying LMCT state observed in the excitation spectrum of this compound. According to the literature, an enhancement of the luminescence properties of mixed-carboxylate complexes can be observed due to a reduction in the polyhedral symmetry of the molecule. In our case, the lowest polyhedral symmetry is observed for the benzoate compound $\mathbf{3}_{\mathbf{Eu}}$ (C_2áµ¥), whereas the polyhedra of our other europium(III) complexes show only minor differences (D_4d). Thus, the effect of polyhedral symmetry on quantum yields in our case cannot be confirmed. The main difference in the crystal structure of type **1** complexes lies in a more developed system of stacking interactions compared to complexes **2** and **3**. This sophisticated system enhances charge delocalization and may lead to an improvement in photoluminescence properties.

According to the literature,[21,22,25] an enhancement of the luminescence properties of mixed-carboxylate complexes can be observed due to a reduction in the polyhedral symmetry of the molecule. In our case, the lowest polyhedral symmetry is observed for the benzoate compound $\mathbf{3}_{\mathbf{Eu}}$ (C_2áµ¥), whereas the polyhedra of our other europium(III) complexes show only minor differences (D_4d) (Table S4†). Thus, the effect of polyhedral symmetry on quantum yields in our case cannot be confirmed. The main difference in the crystal structure of type **1** complexes lies in a more developed system of stacking interactions compared to complexes **2** and **3**. This sophisticated system enhances charge delocalization and may lead to an improvement in photoluminescence properties.

Experimental section

General information

All operations related to the synthesis of complexes were performed in air using commercially available solvents and reagents: MeCN (>99%, KHIMMED), EtOH (96%, FEREIN), 1,10-phenanthroline monohydrate (phen, 99%, "Aldrich-Chemie", Germany), H(pfb) (99%, "P&M Invest"), H(bz) (99%, "Aldrich-Chemie"). Compounds $[Zn(pfb)_2(H_2O)]$,[33] $[Zn(bz)_2(H_2O)_2]\cdot Hbz$,[34] $[Eu_2(pfb)_6(H_2O)_8]\cdot 2H_2O$[35] and $[Ln(bz)_3(H_2O)_4]$ Ln = Eu, Tb[36] were obtained using known methods.

IR spectra of compounds **1–2** were recorded using a Jasco FT/IR-4700 spectrophotometer (China) in the range 550–4000 cm^{-1}. The IR spectra of compounds **3** were recorded using a PerkinElmer Spectrum 65 spectrophotometer (PerkinElmer, Waltham, MA, USA) equipped with a Quest ATR accessory (Specac, Orpington BR5 3FQ, UK) by the attenuated total reflectance (ATR) method in the range 400–4000 cm^{-1}. (abbreviations: w = weak, m = medium, s = strong, sy = symmetric, as = asymmetric, ar = aromatic).

The powder diffraction patterns were obtained using the Bruker D8 Advance diffractometer with a LynxEye detector in

Table 3 Radiative (A_{rad}) and non-radiative (A_{nrad}) rate constants, luminescence lifetimes (τ^{obs}), intrinsic (Q_L^{Ln}) and absolute (Q_L^{Ln}) quantum yields and sensitization efficiency (η_{sens})

Compound		A_{rad}, s^{-1}	A_{nrad}, s^{-1}	τ^{obs}, ms		Q_L^{Ln}, %	Q_L^{Ln}, %	η_{sens}, %
				T = 77 K	T = 300 K			
 (R - phenyl substituent, R` - pentafluorophenyl substituent)	$\mathbf{1_{Tb}}$	—	—	1.85	1.71	—	54	—
$[Tb_2Zn_2(phen)_2(bz)_{5.2}(pfb)_{4.8}]$ 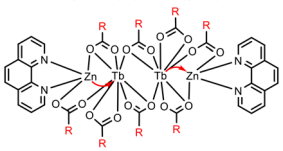 $[Tb_2Zn_2(phen)_2(bz)_{10}]$	$\mathbf{3_{Tb}}$	—	—	1.79	1.69	—	42	—
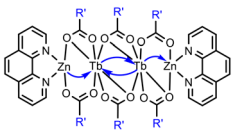 $[Tb_2Zn_2(phen)_2(pfb)_{10}]$	$\mathbf{4_{Tb}}$ [37]				1.83		45	
 $[Eu_2Zn_2(phen)_2(bz)_{5.2}(pfb)_{4.8}]$	$\mathbf{1_{Eu}}$	400	180	1.83	1.71	69	50	73
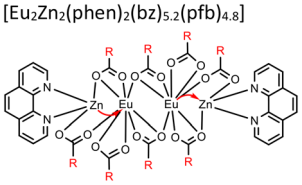 $[Eu_2Zn_2(phen)_2(bz)_{10}]$	$\mathbf{3_{Eu}}$	360	205	1.88	1.78	64	39	61
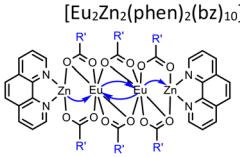 $[Tb_2Zn_2(phen)_2(pfb)_{10}]$	$\mathbf{4_{Eu}}$ [37]	425	100		1.90	81	41	51

Bragg–Brentano geometry. The sample was finely dispersed on a silicon holder with a zero background, λ(CuKα) = 1.54060 Å. The acquired data were refined using the Topas 4 software.[43]

Photoluminescence excitation, emission spectra, and luminescence decays were recorded at room temperature with a Horiba-Jobin–Yvon Fluorolog-QM spectrofluorimeter equipped with a 75 W ArcTune xenon lamp and a Hamamatsu R-FL-QM-R13456 photomultiplier sensitive in the 200–980 nm emission range. The luminescence quantum yield (Q_L^{Ln}) values were measured by the absolute method, employing the same setup equipped with a G8 Spectralon®-covered sphere (GMP SA, Switzerland) and Hamamatsu R13456 photomultiplier. A diffusing screen was mounted inside the sphere to avoid direct irradiation of the detector. The measurements were carried out at ambient temperature. The samples in quartz cells were placed near the center of the sphere. A NIST-traceable 45 W quartz tungsten-halogen bulb emission standard (Oriel) was employed to measure the instrument response function. All QY measurements were repeated at least three times to achieve an experimental error below 15%. The photophysical parameters were calculated *via* Werts' formula.[44]

Synthesis of complexes

Synthesis of $[Ln_2Zn_2(phen)_2(bz)_{5.2}(pfb)_{4.8}]$ (Ln = Eu($\mathbf{1_{Eu}}$); Tb ($\mathbf{1_{Tb}}$)). Compound $[Ln(bz)_3(H_2O)_4]$ (0.145 mmol, Ln = Eu($\mathbf{1_{Eu}}$), Tb ($\mathbf{1_{Tb}}$)) was added to a solution of 0.073 g $[Zn(pfb)_2(H_2O)]$

(0.145 mmol) in 15 mL of MeCN. The reaction mixture was stirred at 70 °C for 10 min, and then phen (0.026 g, 0.145 mmol) was added with stirring. The solution was kept in a sealed vial at room temperature. Colorless crystals suitable for X-ray diffraction studies that precipitated after 7 days were filtered off, washed with cold MeCN (T = 5 °C), and dried in air at 20 °C.

The yield of $\mathbf{1_{Eu}}$ was 0.059 g (44%) based on [Eu(bz)$_3$(H$_2$O)$_4$]. Found, %: C, 46.2; H, 1.8; N, 2.3. For $C_{94}H_{42}Eu_2Zn_2F_{24}N_4O_{20}$ calculated, %: C, 46.3; H, 1.7; N, 2.3. IR (ATR), ν/cm^{-1}: IR-spectrum (ATR; ν, cm^{-1}): 3065 w, 1725 w, 1648 m, 1600 s [as(COO$^-$)], 1561 m [ar(C–C)], 1519 m [C–C], 1490 s [ar(C–C)], 1394 s [sy(COO$^-$)], 1289 w, 1227 w, 1175 w, 1144 w, 1108 m, 991 s [C–F], 932 w, 844 m [ar(C–C)], 768 m, 719 s [ar(C–C)], 643 w, 579 w, 505 w, 441 m, 425 m.

The yield of $\mathbf{1_{Tb}}$ was 0.075 g (62%) based on [Tb(bz)$_3$(H$_2$O)$_4$]·H$_2$O. Found, %: C, 46.1; H, 1.8; N, 2.3. For $C_{94}H_{42}Tb_2Zn_2F_{24}N_4O_{20}$ calculated, %: C, 46.0; H, 1.7; N, 2.2. IR (ATR), ν/cm^{-1}: 1735 w, 1688 w, 1642 m, 1602 m [as(COO$^-$)], 1558 m [ar(C–C)], 1520 m [C–C], 1491 s [ar(C–C)], 1394 s [sy(COO$^-$)], 1290 w, 1176 w, 1149 w, 1107 m, 1069 w, 991 s [C–F], 934 w, 837 w [ar(C–C)], 762 m, 720 s [ar(C–C)], 680 m, 638 w, 576 w, 504 w, 433 m.

Synthesis of [Eu$_2$Zn$_2$(phen)$_2$(bz)$_4$(pfb)$_6$]·4MeCN ($\mathbf{2_{Eu}}$). Compound [Eu$_2$(pfb)$_6$(H$_2$O)$_8$]·2H$_2$O (0.128 g, 0.073 mmol) was added to a solution of 0.068 g [Zn(bz)$_2$(H$_2$O)$_2$]·Hbz (0.145 mmol) in 15 mL of MeCN and 5 mL of EtOH. The reaction mixture was stirred at 70 °C for 20 minutes, after which phen (0.026 g, 0.145 mmol) was added, and the mixture was stirred further. The solution was then kept in a sealed vial at room temperature. After 10 days, colourless crystals suitable for X-ray diffraction studies precipitated were filtered off, washed with cold MeCN (T = 5 °C), and dried in air at 20 °C.

The yield of $\mathbf{2_{Eu}}$ was 0.042 g (22%) based on [Eu$_2$(pfb)$_6$(H$_2$O)$_8$]·2H$_2$O. Found, %: C, 44.9; H, 1.3; N, 3.5. For $C_{100}H_{45}Eu_2Zn_2F_{30}N_7O_{20}$ calculated, %: C, 45.0; H, 1.7; N, 3.7. IR (ATR), ν/cm^{-1}: 3076 w, 1725 w, 1648 m, 1600 m [as(COO–)], 1561 m [ar(C–C)], 1519 m [C–C], 1490 s [ar(C–C)], 1394 s [sy(COO–)], 1289 w, 1226 w, 1175 w, 1144 w, 1108 m, 991 s [C–F], 932 w, 844 w [ar(C–C)], 768 m, 719 s [ar(C–C)], 677 m, 643 w, 579 w, 506 w, 441 m, 425 m.

Synthesis of [Ln$_2$Zn$_2$(phen)$_2$(bz)$_{10}$] (Ln = Eu($\mathbf{3_{Eu}}$); Tb($\mathbf{3_{Tb}}$)). Compound [Zn(bz)$_2$(H$_2$O)$_2$]·Hbz (0.039 g, 0.083 mmol) was added to a solution of [Ln(bz)$_3$(H$_2$O)$_4$]·H$_2$O (0.083 mmol, Ln = Eu($\mathbf{3_{Eu}}$), Tb($\mathbf{3_{Tb}}$)) in 15 mL of MeCN. The reaction mixture was stirred at 70 °C for 10 min, and then phen (0.015 g, 0.083 mmol) was added with stirring. The solution was kept in a sealed vial at room temperature. Colourless crystals suitable for X-ray diffraction studies that precipitated after 10 days were filtered off, washed with cold MeCN (T = 5 °C), and dried in air at 20 °C.

The yield of $\mathbf{3_{Eu}}$ was 0.034 g (41.2%) based on [Zn(bz)$_2$(H$_2$O)$_2$]·Hbz. Found, %: C, 56.1; H, 3.2; N, 3.0. For $C_{94}H_{66}O_{20}N_4Eu_2Zn_2$ calculated, %: C 56.3; H 3.3; N 2.8. IR-spectrum (ATR; ν, cm^{-1}): 3054 w, 2360 w, 2341 w, 1603 s [as(COO$^-$)], 1561 s [ar(C–C)], 1516 w [C–C], 1492 w, 1446 w, 1426 m, 1398 s [sy(COO$^-$)], 1347 w, 1318 w, 1304 w, 1173 w, 1141 w, 1103 w, 1069 w, 1024 w, 847 m [ar(C–C)], 819 w, 807 w, 768 w, 714 s [ar(C–C)], 660 m, 642 w, 618 w, 606 w, 589 w, 578 w, 560 w.

The yield of $\mathbf{3_{Tb}}$ was 0.029 g (34.6%) based on [Zn(bz)$_2$(H$_2$O)$_2$]·Hbz. Found, %: C, 55.8; H, 3.1; N, 2.9. For $C_{94}H_{66}O_{20}N_4Tb_2Zn_2$ calculated, %: C 55.9; H 3.3; N 2.7; IR-spectrum (ATR; ν, cm^{-1}): 3734 w, 2360 m, 2341 m, 1603 s [as(COO$^-$)], 1561 s [ar(C–C)], 1542 m, 1516 w [C–C], 1492 w, 1446 w, 1426 m, 1398 s [sy(COO$^-$)], 1363 w, 1346 w, 1318 w, 1304 w, 1221 w, 1174 w, 1141 w, 1121 w, 1103 w, 1070 w, 1024 w, 983 w, 942 w, 848 m [ar(C–C)], 819 w, 807 w, 768 w, 714 s [ar(C–C)], 679 m, 643 w, 589 w, 574 w, 565 w.

Conclusions

In our studies, benzoate–pentafluorobenzoate [Ln$_2$Zn$_2$(phen)$_2$(bz)$_{5.2}$(pfb)$_{4.8}$] (Ln = Eu ($\mathbf{1_{Eu}}$), Tb ($\mathbf{1_{Tb}}$)) and [Eu$_2$Zn$_2$(phen)$_2$(bz)$_4$(pfb)$_6$]·4MeCN ($\mathbf{2_{Eu}}$) were obtained, in which the simultaneous localization of benzoate and pentafluorobenzoate anions occurs in nearby positions in different ratios. It was found that the use of different metal salts results in complexes with varying compositions, while varying the ratio of the starting reagents only led to the formation of either benzoate or pentafluorobenzoate complexes. In the case of complexes **1** and **2**, it was discovered that the introduction of a heteroanion significantly alters the geometry of the metal framework, the coordination polyhedron of the lanthanide ion, as well as the reorganization of the non-covalent interaction system. Photoluminescence studies revealed that the mixed carboxylate complexes provide better energy transfer to the lanthanide ion than the homoanionic complexes, which leads to a higher quantum yield for complex **1** compared to the analogous benzoate and pentafluorobenzoate complexes **3** and **4**. Thus, the developed approach to the direct enhancement of luminescence by mixing fluorinated and non-fluorinated ligands in the structures of polynuclear {Zn$_2$Ln$_2$} complexes can be used in the design of bright luminescent compounds. For instance, such compounds may be potentially applied as components of emissive layers in organic light-emitting diodes. In this case, future studies on the efficiency and brightness of the electroluminescence and stability of the compounds in the presence of an electric field should be carried out as a logical continuation of this research.

Author contributions

Conceptualization and validation: M. A. S. and J. K. V.; methodology: A. E. B., M. A. S., A. S. C., N. V. G., and E. A. V.; formal analysis: A. E. B., M. A. S., A. S. C., E. A. V., and I. V. T.; investigation: A. E. B., M. A. S., A. S. C., and E. A. V.; writing – original draft preparation: A. E. B., M. A. S., and A. S. C.; writing – review and editing: A. A. S., J. K. V., and I. L. E.; supervision: I. L. E. All authors have read and agreed to the published version of the manuscript.

Data availability

The data supporting this article have been included as part of the ESI.†

CCDC 2343086 ($\mathbf{1}_{Eu}$), 2343087 ($\mathbf{1}_{Tb}$), 2343088 ($\mathbf{2}_{Eu}$), and 2390847 ($\mathbf{3}_{Eu}$) contain the supplementary crystallographic data for this paper.

Conflicts of interest

There are no conflicts to declare.

Acknowledgements

This work was supported by the Russian Science Foundation research grant no. 22-73-10192.

IR spectroscopy, X-ray diffraction, powder X-ray diffraction and CHN analyses of the complexes were performed using the equipment of the JRC PMR IGIC RAS as part of the state assignment of the IGIC RAS in the field of fundamental scientific research. Photophysical measurements were carried out with financial support from the Ministry of Science and Higher Education of the Russian Federation, using the equipment of the Research Center for Molecular Structure Studies, INEOS RAS.

References

1 Q. Liu, S. Z. Ge, J. C. Zhong, Y. Q. Sun and Y. P. Chen, Two novel 2D lanthanide–cadmium heterometal–organic frameworks based on nanosized heart-like Ln6Cd6O12 wheel-clusters exhibiting luminescence sensing to the polarization and concentration of cations, *Dalton Trans.*, 2013, **42**(18), 6314.

2 A. A. Sidorov, N. V. Gogoleva, E. S. Bazhina, S. A. Nikolaevskii, M. A. Shmelev, E. N. Zorina-Tikhonova, *et al.*, Some aspects of the formation and structural features of low nuclearity heterometallic carboxylates, *Pure Appl. Chem.*, 2020, **92**(7), 1093–1110.

3 Q. Liu, F. Wan, L. X. Qiu, Y. Q. Sun and Y. P. Chen, Four 2D Ln–Cd heterometal–organic coordination polymers based on tetranuclear Ln–Cd oxo-cluster with highly selective luminescent sensing of organic molecules and metal cations, *RSC Adv.*, 2014, **4**(51), 27013–27021.

4 H. X. Feng, M. J. Xin and L. W. Sheng, Lanthanide Metalloligand Strategy toward d–f Heterometallic Metal–Organic Frameworks: Magnetism and Symmetric-Dependent Luminescent Properties, *Inorg. Chem.*, 2014, **53**(12), 5922–5930.

5 R. A. Jones, A. J. Gnanam, J. F. Arambula, J. N. Jones, J. Swaminathan, X. Yang, *et al.*, Lanthanide nano-drums: a new class of molecular nanoparticles for potential biomedical applications, *Faraday Discuss.*, 2014, **175**, 241–255.

6 J. Tang, L. Wang, D. Mao, W. Wang, L. Zhang, S. Wu, *et al.*, Ytterbium pentafluorobenzoate as a novel fluorous Lewis acid catalyst in the synthesis of 2,4-disubstituted quinolines, *Tetrahedron*, 2011, **67**(44), 8465–8469.

7 S. M. Yakout, Spintronics: Future Technology for New Data Storage and Communication Devices, *J. Supercond. Novel Magn.*, 2020, **33**(9), 2557–2580.

8 H. Tokoro, A. Namai and O. S. Ichi, Advances in magnetic films of epsilon-iron oxide toward next-generation high-density recording media, *Dalton Trans.*, 2021, **50**(2), 452–459.

9 H. Lian, X. Cheng, H. Hao, J. Han, M. T. Lau, Z. Li, *et al.*, Metal-containing organic compounds for memory and data storage applications, *Chem. Soc. Rev.*, 2022, **51**(6), 1926–1982.

10 J. T. Chen, T. D. Zhou and W. B. Sun, Multifunctional lanthanide-based single-molecule magnets exhibiting luminescence thermometry and photochromic and ferroelectric properties, *Dalton Trans.*, 2023, **52**(15), 4643–4657.

11 F. Manna, M. Oggianu, N. Avarvari and M. L. Mercuri, Lanthanide-Based Metal–Organic Frameworks with Single-Molecule Magnet Properties, *Magnetochemistry*, 2023, **9**(7), 190.

12 T. J. Summers, M. G. Taylor, L. J. Augustine, J. Janssen, D. Perez, E. R. Batista, *et al.*, On the Importance of Configuration Search to the Predictivity of Lanthanide Selectivity, *JACS Au*, 2024, **5**(2), 631–641.

13 J. T. Chen, T. D. Zhou and W. B. Sun, Multifunctional lanthanide-based single-molecule magnets exhibiting luminescence thermometry and photochromic and ferroelectric properties, *Dalton Trans.*, 2023, **52**(15), 4643–4657.

14 D. Parker, J. D. Fradgley and K. L. Wong, The design of responsive luminescent lanthanide probes and sensors, *Chem. Soc. Rev.*, 2021, **50**(14), 8193–8213.

15 Y. J. Chen, C. X. Dou, P. P. Yin, J. T. Chen, X. G. Yang, B. Li, *et al.*, U-type π-conjugated phosphorescent ligand sensitized lanthanide metal–organic frameworks for efficient white-light-emitting diodes, *Dalton Trans.*, 2023, **52**(39), 13872–13877.

16 M. A. Shmelev, R. A. Polunin, N. V. Gogoleva, I. S. Evstifeev, P. N. Vasilyev, A. A. Dmitriev, *et al.*, Cadmium-Inspired Self-Polymerization of {LnIIICd2} Units: Structure, Magnetic and Photoluminescent Properties of Novel Trimethylacetate 1D-Polymers (Ln = Sm, Eu, Tb, Dy, Ho, Er, Yb), *Molecules*, 2021, **26**(14), 4296.

17 Y. Meng, Y. Cheng, X. Yang, C. Wang, K. Yang and D. Schipper, Construction of a Zn(II)–Eu(III) Nanoring with Temperature-Dependent Luminescence for the Qualitative and Quantitative Detection of Neopterin as an Inflammatory Marker, *Inorg. Chem.*, 2024, **63**(16), 7199–7205.

18 M. A. Shmelev, Yu. K. Voronina, N. V. Gogoleva, A. A. Sidorov, M. A. Kiskin, F. M. Dolgushin, *et al.*, Influence of the steric properties of pyridine ligands on the structure of complexes containing the {LnCd2(bzo)7} fragment, *Russ. Chem. Bull.*, 2020, **69**(8), 1544–1560.

19 Y. Zhang, W. Feng, H. Liu, Z. Zhang, X. Lü, J. Song, *et al.*, Photo-luminescent hetero-trinuclear Zn2Ln (Ln = Nd, Yb, Er or Gd) complexes based on the binuclear Zn2L precursor, *Inorg. Chem. Commun.*, 2012, **24**, 148–152.
20 F. Q. Song, H. Cheng, N. N. Zhao, X. Q. Song and L. Wang, Anion-Dependent Structure and Luminescence Diversity in Zn II -Ln III Heterometallic Architectures Supported by a Salicylamide-Imine Ligand, *Inorg. Chem.*, 2021, **60**(22), 17051–17062.
21 N. B. D. Lima, A. I. S. Silva, S. M. C. Gonçalves and A. M. Simas, Synthesis of mixed ligand europium complexes: Verification of predicted luminescence intensification, *J. Lumin.*, 2016, **170**, 505–512.
22 N. B. D. Lima, A. I. S. Silva, V. F. C. Santos, S. M. C. Gonçalves and A. M. Simas, Europium complexes: choice of efficient synthetic routes from RM1 thermodynamic quantities as figures of merit, *RSC Adv.*, 2017, **7**(34), 20811–20823.
23 M. A. Shmelev, G. N. Kuznetsova, N. V. Gogoleva, F. M. Dolgushin, Yu. V. Nelyubina, M. A. Kiskin, *et al.*, Heteroleptic cadmium(II) and terbium(III) pentafluorobenzoate–benzoate and pentafluorobenzoate-2-furancarboxylate compounds, *Russ. Chem. Bull.*, 2021, **70**(5), 830–838.
24 H. L. Wang, X. F. Ma, H. H. Zou, K. Wang, B. Li, Z. L. Chen, *et al.*, Mixed chelating ligands used to regulate the luminescence of Ln(III) complexes and single-ion magnet behavior in Dy-based analogues, *Dalton Trans.*, 2018, **47**(44), 15929–15940.
25 N. B. D. Lima, S. M. C. Gonçalves, S. A. Júnior and A. M. Simas, A Comprehensive Strategy to Boost the Quantum Yield of Luminescence of Europium Complexes, *Sci. Rep.*, 2013, **3**(1), 2395.
26 L. L. L. S. Melo, G. P. Castro and S. M. C. Gonçalves, Substantial Intensification of the Quantum Yield of Samarium(III) Complexes by Mixing Ligands: Microwave-Assisted Synthesis and Luminescence Properties, *Inorg. Chem.*, 2019, **58**(5), 3265–3270.
27 J. K. Voronina, D. S. Yambulatov, A. S. Chistyakov, A. E. Bolot'ko, L. M. Efromeev, M. A. Shmelev, *et al.*, Influence of the Arene/Perfluoroarene Ratio on the Structure and Non-Covalent Interactions in Crystals of Cd (II), Cd(II)-Tb(III) and Cu(II) Compounds, *Crystals*, 2023, **13**(4), 678.
28 C. E. Smith, P. S. Smith, R. L. l. Thomas, E. G. Robins, J. C. Collings, C. Dai, *et al.*, Arene-perfluoroarene interactions in crystal engineering: structural preferences in polyfluorinated tolans, *J. Mater. Chem.*, 2004, **14**(3), 413–420.
29 L. Wang, J. Deng, M. Jiang, C. Zhen, F. Li, S. Li, *et al.*, Arene–perfluoroarene interactions in molecular cocrystals for enhanced photocatalytic activity, *J. Mater. Chem. A*, 2023, **11**(21), 11235–11244.
30 J. C. Collings, K. P. Roscoe, E. G. Robins, A. S. Batsanov, L. M. Stimson and J. A. K. Howard, *et al.*, *Arene-perfluoroarene interactions in crystal engineering 8: Structures of 1 : 1 complexes of hexafluorobenzene with fused-ring polyaromatic hydrocarbonsyz*, in *New Journal of Chemistry*, Royal Society of Chemistry, 2002, pp. 1740–1746.
31 X. H. Zhou, J. Luo, S. Huang, T. D. Kim, Z. Shi, Y. J. Cheng, *et al.*, Supramolecular self-assembled dendritic nonlinear optical chromophores: Fine-tuning of arene-perfluoroarene interactions for ultralarge electro-optic activity and enhanced thermal stability, *Adv. Mater.*, 2009, **21**(19), 1976–1981.
32 T. Itoh, M. Kondo, M. Kanaike and S. Masaoka, Arene-perfluoroarene interactions for crystal engineering of metal complexes: Controlled self-assembly of paddle-wheel dimers, *CrystEngComm*, 2013, **15**(31), 6122–6126.
33 M. A. Shmelev, Yu. K. Voronina, N. V. Gogoleva, M. A. Kiskin, A. A. Sidorov and I. L. Eremenko, Synthesis and Crystal Structure of $\{Eu_2IIICd_2\}$, $\{Tb_2IIICd_2\}$ and $\{Eu_2IIIZn_2\}$ Complexes with Pentafluorobenzoic Acid Anions and Acetonitrile, *Russ. J. Coord. Chem.*, 2022, **48**(4), 224–232.
34 B. T. Usubaliev, P. S. Abdurakhmanova, M. K. Munshieva and D. M. Ganbarov, Clathrate $[Zn(C6H5COO)2(H_2O)2] \cdot 2CH_3COOH$: Synthesis and crystal structure, *Russ. J. Coord. Chem.*, 2010, **36**(11), 865–869.
35 S. V. Larionov, L. A. Glinskaya, T. G. Leonova, R. F. Klevtsova, E. M. Uskov, V. E. Platonov, *et al.*, Luminescence properties of complexes Ln(Phen)(C6F5COO)3 (Ln = Tb, Eu) and $Ln(C6F5COO)3 \cdot nH_2O$ (Ln = Tb, n = 2; Ln = Eu, n = 1). Structures of the $[Tb2(H_2O)8(C6F5COO)6]$ complex and its isomer in the supramolecular compound $[Tb2(H_2O)8(C6F5COO)6] \cdot 2C6F5COOH$, *Russ. J. Coord. Chem.*, 2009, **35**(11), 798–806.
36 M. S. Khiyalov, I. R. Amiraslanov, F. N. Musaev and K. S. Mamedov, Structural and thermographic investigation of dysprosium (3) pentaaquobenzoate, *Koord. Khim.*, 1982, **8**(4), 548.
37 M. A. Shmelev, M. A. Kiskin, J. K. Voronina, K. A. Babeshkin, N. N. Efimov, E. A. Varaksina, *et al.*, Molecular and Polymer Ln2M2 (Ln = Eu, Gd, Tb, Dy; M = Zn, Cd) Complexes with Pentafluorobenzoate Anions: The Role of Temperature and Stacking Effects in the Structure; Magnetic and Luminescent Properties, *Materials*, 2020, **13**(24), 5689.
38 M. Yin and J. Sun, Synthesis and characterization of two tetranuclear heterometallic Tb(III)–Zn(II) complexes, *J. Coord. Chem.*, 2005, **58**(4), 335–342.
39 R. K. R. Jetti, R. Boese, P. K. Thallapally and G. R. Desiraju, Five New Pseudopolymorphs of *s ym* -Trinitrobenzene, *Cryst. Growth Des.*, 2003, **3**(6), 1033–1040.
40 D. Sharada, A. Saha and B. K. Saha, Charge transfer complexes as colour changing and disappearing–reappearing colour materials, *New J. Chem.*, 2019, **43**(20), 7562–7566.
41 M. A. Shmelev, J. K. Voronina, M. A. Evtyukhin, F. M. Dolgushin, E. A. Varaksina, I. V. Taydakov, *et al.*, Synthesis, Structure and Photoluminescence Properties of Cd and Cd-Ln Pentafluorobenzoates with 2,2′:6′,2′-Terpyridine Derivatives, *Inorganics*, 2022, **10**(11), 194.

42 L. N. Puntus, K. A. Lyssenko, M. Yu. Antipin and J. C. G. Bünzli, Role of Inner- and Outer-Sphere Bonding in the Sensitization of Eu III -Luminescence Deciphered by Combined Analysis of Experimental Electron Density Distribution Function and Photophysical Data, *Inorg. Chem.*, 2008, **47**(23), 11095–11107.
43 N. V. Y. Scarlett and I. C. Madsen, *Powder Diffr.*, 2006, **21**(4), 278.
44 M. H. V. Werts, R. T. F. Jukes and J. W. Verhoeven, The emission spectrum and the radiative lifetime of Eu^{3+} in luminescent lanthanide complexes, *Phys. Chem. Chem. Phys.*, 2002, **4**, 1542–1548.